Swirl motion effects on flame dynamic of pulverized olive cake in vertical furnace

A. Elorf[1*], N. Mrad-koched[1], S.Bostyn[1], B. Sarh[1], I. Gökalp[1], B. Izrar[1], J. Chaoufi[2]
[1] ICARE-CNRS-Université d'Orléans, 1C, Avenue de la Recherche Scientifique, 45071 Orléans Cedex 2, France
[2]LETSMP, Département de physique, Université Ibn Zohr, 80000 Agadir, Maroc

1 Introduction

Biomass is an important fuel for heating and power generation because it is a readily available renewable energy source that reduces carbon dioxide emissions. An understanding of the physical and chemical processes involved in biomass combustion is important for any application in which biomass combustion is required, including stoves, boilers, and large-scale burners [1-2]. Substituting for traditional fossil fuel with biomass large scale combustion facilities is not only of significant importance for meeting society's energy needs, but can also make a huge contribution towards the reduction of greenhouse gases emitted into the atmosphere. Furthermore, the development of new technologies for utilization of biomass raises new opportunities for economic re-vitalization and growth [3-5].

Olive Cake (OC), which is a waste of olive oil-mill, is an important biomass generated in Mediterranean countries. OC is available in large amounts at a very low cost. Vegetable oils and OC can be considered as alternative fuels, which do not contain sulfur [6]. OC actually is a waste and like other wastes can cause problems if suitable and acceptable disposal measures are not taken. Efficient use of OC in energy production solves the two problems in one step: clean energy production and acceptable disposal of olive-mill wastes. OC can be burned alone or can be combined with other combustible materials, like low calorific value lignite coals. Morocco is rich in olive trees. Annually, about 1.5 million tons of olive is used in olive oil production and approximately 675,000 tons of OC are produced. The calorific value (LHV) of this OC is about 12,500– 22,000 kJ/kg. It is comparable with the calorific values of wood and soft coal, which are 17,000 and 23,000 kJ/kg, respectively. The sulfur content of OC is about 0.05– 0.1 wt%. Therefore, it is of prime importance to be able to burn this waste in producing clean energy in the regions where olive trees are raised. However, an appropriate technology must be employed to avoid the production of pollutants and other problems while maximizing process efficiency [6-7].

Modeling may help to increase our understanding of the combustion processes taking place. Not all the relevant phenomena in a combustion system are described in depth, but CFD calculations give an approximate overview of the system, helping to troubleshoot and fine-tune the system's operation, as well as give assistance when dealing with new designs. At present, there are still only a very few numerical simulations of biomass combustion systems using detailed models for both the bed and gas phases [8-9].

In this work, the development and application of a CFD model for pulverized olive cake combustion is presented. The Discrete Phase Model (DPM) of the commercial CFD software FLUENT 14 available in the laboratory, originally developed for the combustion of pulverized coal, was investigated regarding its capability to predict pulverized biomass combustion in general and especially olive cake presented in this paper. For burning biomass in particle form, the particles were described as a discrete phase in great number of works, for

this, DPM is used for tracks the motion of individual (discrete) particles. Note that the same principles apply whether the object is a solid particle, or, a liquid droplet. Toporov et al [13] studied the detailed numerical and experimental investigation of pulverized coal swirl flame. The combustion tests were performed in a vertical pilot-scale furnace (100kw). Comparison between measurements and simulation has shown the validity of the numerical method. Before starting our simulations of olive cake, it's interesting to assess the methodology used. For that it's evident to simulate existing data in the literature.

The first part in this study is to compare the model used in current numerical simulation with the experimental results obtained by Toporov et al [13]. The current RANS results give good agreement to experimental data of axial velocity profiles for two different axial distances close to the burner exit. The second part is to examine the combustion of olive cake with various inlet flow conditions (with and without swirl motion). Two cases are studied for the inlet conditions. First, without swirl motion (Ja) and second, with swirl motion (Js). The numerical approach is based on Reynolds Average Navier-Stokses (RANS) equations. The OC particles are injected perpendicularly to the furnace axis near the lower base. This injection mode increases the particle residence time in the furnace. The OC thermal characteristics are determined from thermogravimetric analysis.

2 Governing equations

2.1 Continuous gas phase (gas flow)

The gas phase transport is described by the standard equations of fluid dynamics: the continuity, momentum, energy transport and species transport equations. A Fluent standard k-ε model was chosen for the turbulence model, as this is the most appropriate model when turbulence transfer between phases plays an important role in gasification in the combustion chambers. For the chemical reaction modeling, the PDF/mixture fraction model is used. In this approach equations for two conserved scalars (f_{fuel}: the fuel or char mixture fraction and f_{sec}: the mixture fraction of the volatiles) and their variance are solved, and individual component concentrations are derived from the predicted mixture fraction distribution. In addition, the reaction is assumed to be mixing limited (local chemical equilibrium conditions prevail). For the mixture fraction approach, the equilibrium chemistry PDF model is used. The equilibrium system for biomass (OC) combustion consists of 20 species (C, C(s), H, H_2, O, O_2, N, N_2, CO, CO_2, OH, H_2O, CH_4, C_2H_2, CH_3, HO_2, C_2H_4, C_2N_2 and C_2H_6). Being a conserved scalar quantity, the value of f at each point in the flow domain is computed through the solution of the conservation equation for mean (time-averaged) value of f in the turbulent flow field, f [10]:

$$\frac{\partial}{\partial x_i}(\rho u_i f) = \frac{\partial}{\partial x_i}\left(\frac{\mu_t}{\sigma_t}\frac{\partial \overline{f}}{\partial x_i}\right) + S_M$$

In addition to solving the conservation equation for the mean mixture fraction, a conservation equation for the mixture fraction variance, f'^2 is also solved:

$$\frac{\partial}{\partial x_i}(\rho u_i \overline{f'^2}) = \frac{\partial}{\partial x_i}\left(\frac{\mu_t}{\sigma_t}\frac{\partial \overline{f'^2}}{\partial x_i}\right) + C_g \mu_t \left(\frac{\partial \overline{f}}{\partial x_i}\right)^2 - C_d \rho \frac{\varepsilon}{k}\overline{f'^2}$$

The values of constants σ_t, C_g and C_d in this equation will be taken depending on simulations and situation, respectively. If a secondary stream is included in a non-adiabatic system, the instantaneous values will depend on the instantaneous fuel mixture fraction, fuel, the secondary partial fraction, p_{sec} and the enthalpy, H

$$\Phi_i = \Phi_i^*\left(f_{fuel}, p_{\sec}, H^*\right) \quad \text{With} \quad H^* = \sum_{i'} m_{i'} H_{i'} = \sum_{i'} m_{i'}\left[\int_{T_{ref_{i'}}}^{T} C_p + h_{i'}^0(T_{ref_{i'}})\right]$$

More details about solution could be referred from Ref. [11]

2.2 Equation for particle motions

Olive cake particles were modeling using the Discrete Phase Model (DPM) approach. The trajectory of the discrete particle was calculated by integrating the force balance on the particle as in the motion equation [11]:

$\frac{d\vec{u}_p}{dt} = F_D(\vec{u}+\vec{u}_p) + \vec{g}(\rho_p - \rho)/\rho_p$ Where $F_D(\vec{u}+\vec{u}_p)$ is the drag force per unit particle mass; u is the fluid phase velocity; u_p is the particle velocity; ρ is the fluid density and ρ_p is the particle density. The drag force has an important effect on the trajectory of discrete particles.

2.3 Radiation model

The radiation process influences the heat transfer rate in the furnace units. The Fluent following models are applicable: Discrete ordinates model, P-1 model, Rosseland model and Discrete transfer radiation model. In this study, the P-1 radiation model is used to calculate the radiation heat source term in the energy equation for the particle [12]. This model should typically be used for optical thicknesses large than 1. We have selected this model because it is accurate for combustion applications wherein the optical thickness is large, it can easily be applied to complicated geometries, it consumes little central processing unit (CPU) time and in the literature it's validated in several studies to simulate the radiation model.

3 Test methodology case

Toporov et al [13] studied pulverized coal combustion in vertical furnace with a length of the combustion chamber 2100 *mm* and the inner diameter of 400 *mm* with the swirl burner located on top of the combustion chamber. The particles size is 0.9-123 *µm* enters the combustion chamber together with the primary air. Mass flow rate of the fuel is 6.5 *kg/h* and gas is 17.6 *kg/h.* Secondary gas inlet mass flow rate is *26.6kg/h* and is highly swirled with the swirl number of 1.2, defined as a ratio of tangential velocity to axial one. In this case we compare the results obtained in the experiment of Toporov and the current numerical study.

Figure 1 shows comparison of axial velocity profiles obtained in the experiment of Toporov et al and the current numerical simulation at two axial distances from the burner exit. The numerical simulation results are very similar for the second axial distance (figure 1 (b)) and give a good agreement to experimental data closed to the burner exit (figure 1 (a)).

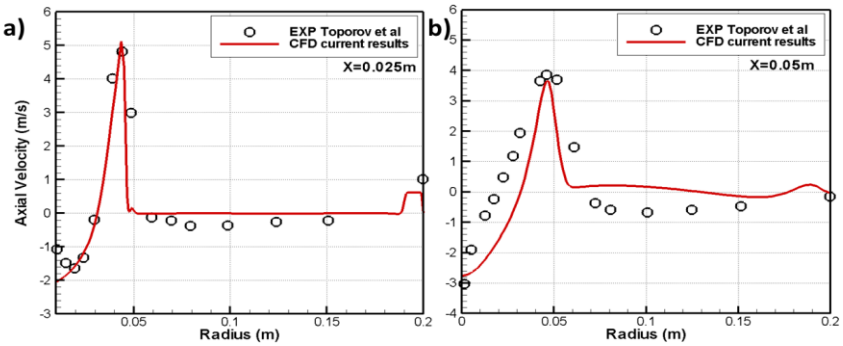

Figure 1. Axial velocity at axial distance from the burner 0.025 m (a) and 0.05 m (b)

4 Numerical method

4.1 Geometry and mesh construction:

A schematic view of the cylindrical combustion chamber is shown in Figure 2. The combustion chamber is a cylindrical tube with inner diameter of 500 *mm* and total length of 1500 *mm.* The air inlet diameter d=*80 mm* is divided in two diameters primary air inlet of which the diameter is equal to 50 *mm*, and secondary, coaxial oxygen inlet with outside diameter 80 *mm* and internal diameter 52 *mm*. In this study secondary inlet is the air.

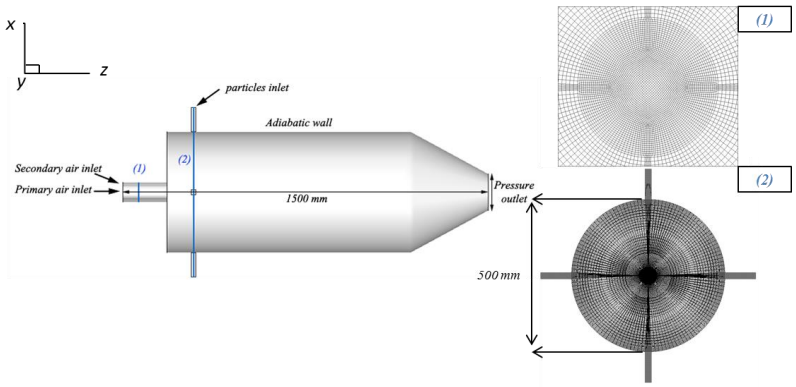

Figure 2. Geometry and computational mesh

4.2 Grid sensitivity analysis

Owning to the symmetrical geometry of the present furnace, only one quarter of the furnace was modeled to minimize the rate calculation.

Three computational structured grids (coarse, medium and a fine) are designed, as presented in Table 1. The difference in these three meshes is mainly due to different grid resolution requirements in order to have higher resolution in the injection pipe and in the flame region.

A grid convergence study has been conducted for three meshes discussed in Table 1. This analysis is done by simulating the non-reacting flow using the Standard *k-ε* model.

Table 1. Summary of grid refinement

Grid refinement	**Total number of cells**
Coarse	1956384
Medium	3960000
Fine	5460528

At the inlet the mass flow rate of air inlet is $\dot{m}_{air} = 7.38\ g/s$. A ratio of axial and tangential velocities *w/u=0.9* is introduced to give the flow the desired swirling velocity for (Js) case. In the burner the flame operates with a perfect mixing of fuel and air, for a global equivalence ratio $\phi = 0.58$ at atmospheric pressure, the OC mass flow rate calculated is $\dot{m}_{PO} = 0.561 g/s$.

Comparison of the mean axial velocity radial profiles in the burner is presented in Figure 3. Both profiles of fine and medium grids show the same trend in all axes z/d presented.

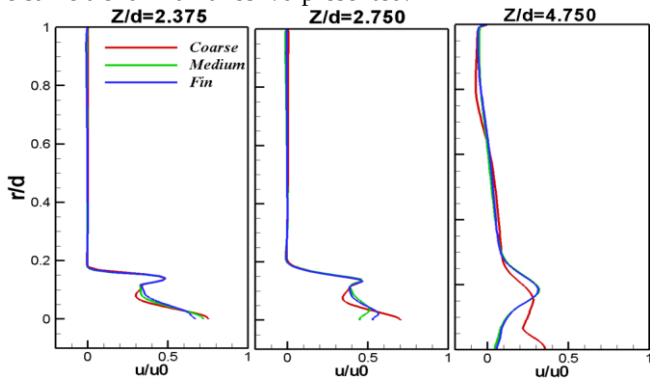

Figure 3. Grid-independence test in axial velocity at several locations.

The profiles of the coarse grid illustrate a significant difference in the location of axial velocity peaks. Therefore, the medium grid was chosen for all calculation in the present study.

5 Results

Tables 2 show the proximate and ultimate analysis of the fuel used in this study. To determine experimentally the thermal characteristics of OC it has been used ATG (Thermogravimetric Analysis) available in the laboratory. This technique allows access to percentages volatile matter, fixed carbon and ash samples of OC. The calorific value is calculated also in the laboratory using the bomb calorimeter. The experimental lower heating value of OC is 19.8 MJ/Kg.

Table2. Proximate and ultimate analysis of the OC used

Proximate Analysis (Wt%, dry) -DAF		Ultimate analysis(Wt %, dry)	
Volatile Matter	64	Carbon	59
Fixed Carbon	23.2	Hydrogen	8.5
Ash	6.5	Nitogen	1.5
Moisture	6.3	Sulphur	0
		Oxygen	31

Fuel particle distribution is inserted into computational domain as Rosin-Rammler distribution. The particles size range are a minimal diameter D_{min}*=70 µm*; a maximal diameter D_{max}*=200 µm* and a mean diameter D_{mean}*=100 µm.*

The streamline plot on the x-z plane of both (Ja) and (Js) cases is presented in Figure 4. It can be seen that the flow topology is deferent for each case, because of the effect of the swirling motion. Three zones are noticed: the recirculation zones (red dot), the horseshoe (green dot) and the separation node (purple cross mark) in both cases. In (Ja) case there is one recirculation zone which takes its shape from the neighboring wall and it is far of the burner inlet, but in (Js) case there is two recirculation zones which are a result of the swirling flow expansion and they are close to the burner inlet. A fourth zone named a stagnation point (blue plus mark) which exists only in the (Js) case which appears from the shear between the two recirculation zones.

Figure 5 illustrates the axial velocity contours (a) and kinetic energy (b) in the burner for both (Ja) and (Js) cases. It is shown that the negative velocity region near the wall is decreased in the swirling jet flow in comparison with the axial jet flow. The maximum axial velocity along the burner is located in the center region for the (Ja) case, that makes the kinetic energy of the flow concentrated only in the center. Regarding the (Js) case, the swirling jet makes the maximum axial velocity located far of the center region, which leads to distributing the kinetic energy of the flow in the radial direction, and this will affect the flame location to be close to the flow inlet.

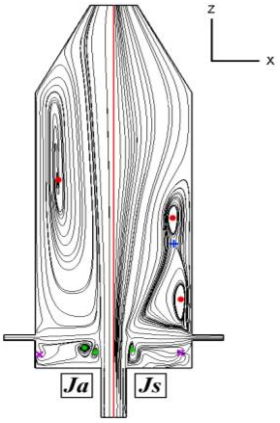

Figure 4. The streamline: Left without swirl, right with swirl

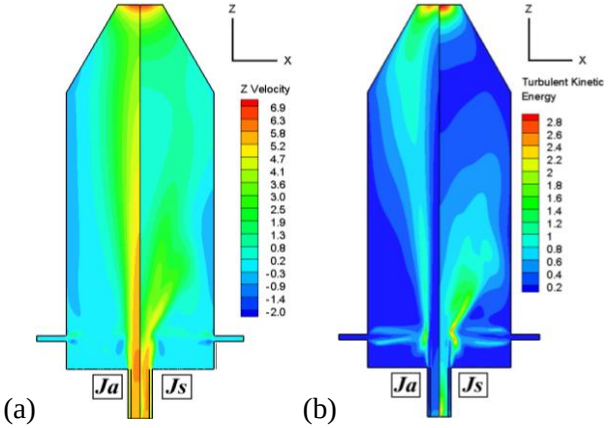

Figure 5.a) Axial velocity contours, b) Kinetic energy contours : Left without swirl, right with swirl

Figure 6 shows the predicted spatial distribution of temperature along the burner (a), in addition to the centerline (X/d=0) and in vertical cross section that contains the maximum temperature (X/d=1.875) profiles temperature (b) for both (Ja) and (Js) cases. It is shown that the maximum temperatures are located in the recirculation zones, which confirms that those zones play the role of the flame holder. In the (Js) case the maximum temperature is to higher and closes the inlet flow entry, unlike the (Ja) case that predicts a lower temperature values and far of the inlet flow entry. Regarding the centerline (X/d=0) temperature, it starts with a constant value for both cases until Z/d = 5. In X/d=1.875 we note that the maximum temperature is located at Z/d=7 and Z/d=12 respectively for (Js) and (Ja) cases. Then, it becomes higher for the (Js) case comparing with (Ja) case and this is due to the high axial velocity in the center region for the (Ja) case which makes the flame blowing out.

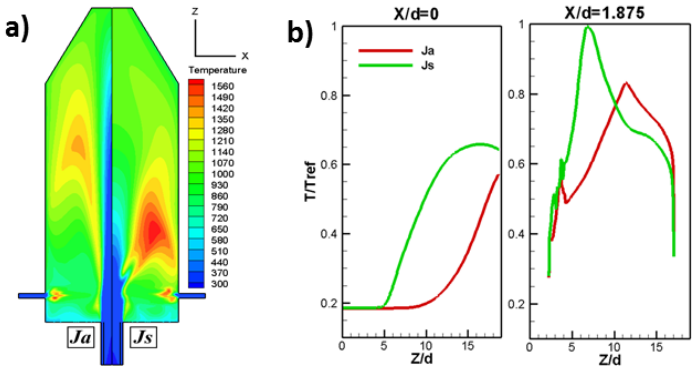

Figure 6. a) Temperature contours: Left without swirl, right with swirl, b) Gaz temperature along furnace axis (X/d=0) and along maximum furnace temperature (X/d=1.875)

Figure 7 presents the radial profiles of CO_2 mass fraction in several longitudinal locations. The maximum CO_2 mass fraction value locates close to the burner inlet (Z/d=3.125) far both (Ja) and (Js) cases. The CO_2 mass fraction decreased when it is far of the inlet. It is shown that the (Js) case provide less CO_2 concentration in comparison with (Ja) case. Furthermore the swirling motion helps to reduce the CO_2 emissions.

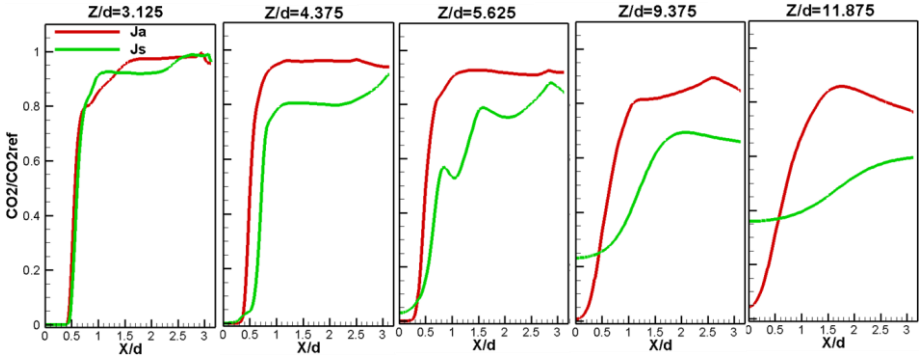

Figure 7. CO_2 mass fraction radial profiles for (Ja) and (Js) cases

6 Conclusion

This work summarized the CFD modeling tool to study combustion of pulverized OC in vertical furnace with various inlet flow conditions. A comparison was made between (Ja) and (Js) cases for, flow topology, velocity contours, temperature distribution and species concentrations profiles in several location along the burner. The results present that the flame is more stabilized and closer to the inlet for the (Js) case in comparison with (Ja) case, and reaches its maximum value of 1560 K. There is evidence that CFD can be used as a powerful tool to predict characteristics of fuels and solid biomass during combustion.

Acknowledgements

The authors wish to acknowledge the financial support from Region Centre (Project VERA).

References

[1] Collazo J, Porteiro J. (2012). Numerical modeling of the combustion of densified wood under fixed-bed conditions. Fuel. 93:149.

[2] Al-attab KA, Zainal ZA. (2011). Design and performance of a pressurized cyclone combustor (PCC) for high and low heating value gas combustion. Applied Energy. 88:1084.

[3] Chungen Yin, Lasse AR, Søren KK. (2008). Grate-firing of biomass for heat and power production. Progress in Energy and Combustion Science. 34: 725.

[4] Xinhui Z, Mohsen G, Albert R. (2013). Numerical modeling of co-firing a light density biomass, oat (Avena sativa) hulls, and chunk coal in fluidized bed boiler. Biomass and bioenergy. 56:239.

[5] Ravi IS, Anders B, Mikko H. (2013). CFD modeling to study fluidized bed combustion and gasification. Applied Thermal Engineering. 52:585.

[6] Hu¨seyin T, Aysel TA, Ali D. (2003). Olive cake combustion in a circulating fluidized bed. Fuel. 82:1049.

[7] Aysel TA, Hu¨seyin T. (2004). Co-combustion of olive cake with lignite coal in a circulating fluidized bed. Fuel. 83:859.

[8] Janarjeh I, Sharh MAL. (2013). Numerical and experimental investigation of downdraft gasification of wood chips. Energy Conversion and Management. 65:783.

[9] James EM, Mathieu S, Mark J, Eilberto T.(2009). CFD Moedelling of pulverized coal combustion in a rotary lime kiln. 7th Int. Con. on CFD in the Minerals and Process Industries.

[10] Ravi IS, Anders B, Mikko H. (2013). CFD modeling to study fluidized bed combustion and gasification. Applied Thermal Engineering. 52 : 585

[11] ANSYS® Academic Research. Release 14.0. Help System. FLUENT User Guide. ANSYS Inc.

[12] Gautham K, Rajesh R, Philip JS. (2006). Parallelization of the P-1 Radiation Model. Numerical Heat Transfer, Part B: Fundamentals. 49:1.

[13] Toporov D, Bocian P, Heil P, Kellermann A, Stadler H, Tschunko S, Forster M, Kneer R. (2008). Detailed investigation Of a pulverized fuel swirl flame in CO_2/O_2 atmosphere. Combustion and flame. 155:618.